UNIVERSITY OF CALIFORNIA
Los Angeles

Pneumatics powered by liquid nitrogen for robotics applications

A thesis submitted in partial fulfillment
of the requirements for the degree Master of Science
in Mechanical Engineering

by

DaEun Park

2016

ABSTRACT OF THE THESIS

Pneumatics powered by liquid nitrogen
for robotics applications

by

DaEun Park

Master of Science in Mechanical Engineering
University of California, Los Angeles, 2016
Professor Dennis Hong, Chair

Despite its potential as a high efficiency power-actuation mechanism, cryogen powered pneumatics system have been one of the least popular choice for robotic engineers due to its nonlinearities and other modeling complexities. For this thesis, an ideal model of liquid nitrogen powered pressurized vessel for pneumatic muscle actuator application with minimal complexity has initially been developed. Few control algorithms have been tested to investigate the robustness of the pneumatic force generation in creating stable profiles of output pressure of pressurized vessel. Then finally, a more realistic, low-cost, portable, increased-safety solution, both in terms of physical size and control platform, has been provided to meet the practical needs in the field of advanced robotics.

The thesis of DaEun Park is approved.

Adrienne Lavine

Tetsuya Iwasaki

Dennis W. Hong, Committee Chair

University of California, Los Angeles

2016

Table of Contents

List of Figures

Acknowledgement

I would like to thank all my committee members:

Prof. Hong for overall guidance on the project,

Prof. Lavine for her advices on thermodynamics, and

Prof. Iwasaki for his clarifications on controls theory.

I would also like to thank my colleagues:

Lin Xuan for his help on fluid mechanics, and

Joshua Hooks for his help on controller simulation.

Motivation

Anyone who has gone through the development process of high power demand robotic platform, such as an industrial robot or a humanoid robot, would agree that one of the most important design criteria is the energy conservation. For example, the adult-size soccer playing humanoid robot, THOR-RD (short for Tactical Hazardous Operations Robot – Rapid Deployment) can be run on a rechargeable Li-Po battery (11000 Amp-hour), untethered. Even with the carefully planned locomotion strategies and optimized trajectories, it can barely last 45 minutes to perform the tasks in playing soccer. Humanoid robotics engineers have been increasingly recognizing the need for an intelligent strategy to handle the power generation, so that every meaningful behavior of the robot is carried out in an energy efficient way.

Our goal is to develop a robust pneumatic actuation system that allows us to exploit this technology in the field of robotics. For the first part, we aim to develop a suitable control algorithm for a pneumatic robot platform that utilizes liquid nitrogen (LN2) as its source of energy. For the second part, we aim to design and manufacture a pressure vessel that can generate a range of desired torque for typical pneumatic muscle actuators. We have obtained preliminary data for output pressure from the LN2 vessel that are essential in designing various types of pneumatic muscle.

Thermal Energy Storage (TES) is a technology that reserves energy by heating or cooling the thermal storage medium for later uses [5]. The ever-growing energy demand in the midst of depleting fossil fuel resources and the raised awareness on mitigating the environmental burden (greenhouse gas emissions and climate change) are the major motivation behind developing alternative renewable energy sources and sustainable energy storage technology. TES is one of the alternative technologies that provides a few environmental advantages over other alternatives,

such as electrochemical batteries, which are known to cause heavy metal pollution and recycling complication.

Cryogenic energy storage is a type of TES technology, which employs cryogenic medium as a heat sink and the atmosphere or other working fluids as a heat source. The cold temperature storage medium can deliver more valuable energy (low entropy energy, or exergy) than the high temperature storage media, according to the 2nd law of thermodynamics [3]. This technology has attracted many researchers, primarily due to its ability to carry high-density exergy, and the elemental abundance of many liquefied inert gas species, including hydrogen, methane, and nitrogen.

There are many ways to extract energy from cryogen. First is the direct expansion method, in which the cryogens are pumped to a high pressure, brought up to the room temperature by atmospheric heat, and followed up by volume expansion to generate power. Second is indirect heating via a Rankine cycle, in which the cryogenic exergy is transferred to the working fluid and the temperature difference between the cryogen and ambient makes the working fluid generate power. Third is via Brayton cycle, in which the cryogen cools down and pressurizes the inlet gas of a compressor. The high pressure, low temperature outlet gas is heated by the ambient and followed up by volume expansion in the expander to generate power. Cryogenic heat engines with one or two of the three mechanisms described above are developed to put this technology into use. Many researchers have published their studies about implementing cryogenic engines into an existing platform. Two of which are different types of LN2 driven automobiles: one using the closed Rankine cycle [2], and the other one using the closed Brayton cycle [4]. Amongst the cryogens, LN2 has gained an extra attention from the researchers because it has higher thermal exergy than other liquefied inert gas species, and produces zero chemical exergy. Given its potential as a combustion free fuel, LN2 heat engine has followed the path of developing zero emission vehicles, and other applications where high power turbine engine is needed. However, these studies have only been

analyzed over a limited number of applications, and yet to be extended to other applications that also require high-energy consumption, such as robotics. Inviting ourselves into this new realm of technology, we are inevitably faced with many challenges, including but not limited to, difficulties in control design due to nonlinearities in turbulent fluid flow (with Reynolds number expected to be in the order of tens of thousands), randomness in thermodynamic plant, and time delay in energy supply from the engine to the actuator.

Objectives

The direct expansion method is used for our engine. Our heat engine comprises of two parts: the liquefied inert gas reservoir, and the heat exchange vessel, where the gas expansion followed by phase change occurs. To avoid design complications, there is no pursuit on energy time shifting mechanism that, if implemented, could have optimized the supply operations based on the demand. Instead, we assume an infinite supply of LN2 and that the vessel quickly turns into a compressed gas reservoir that supplies to the pneumatic actuator upon LN2 injection. For the purpose of our project, we consider that this conversion happens instantaneously because the time constant of this thermodynamic process is very small compared to the mechanical time constant of the pneumatic actuator (Appendix B). In other words, we ignore the thermodynamic time delay from the cryogenic injection (to the engine) to the pressurized gas supply (to the actuator), which lets us have one less pressure supply nonlinearity in modeling the system.

Controller simulation

Set-up

Figure 1 shows the design of liquid nitrogen powered pneumatics. There is an inlet valve to control the high-pressure (p0) nitrogen gas flow into the left chamber. Also, there's an outlet valve, which connects the chamber with atmosphere, with pressure p_{atm}. The right chamber is connected to another pressurized reservoir with $p0$'. In

order to control the position of piston, we have $p_{atm} < p0' < p0$. Therefore, if we turn up the inlet valve, the pressure inside the left chamber will rise, and the piston will go right, and vice versa. However, when we turn on the valve, the pressure inside the chamber doesn't reach a steady value immediately. If we suddenly turn on the valve, the pressure difference will cause a flow into the chamber, which led to a pressure increase. As the pressure reaches its steady value, the flow eventually settles down. Thus a dynamic process will be observed.

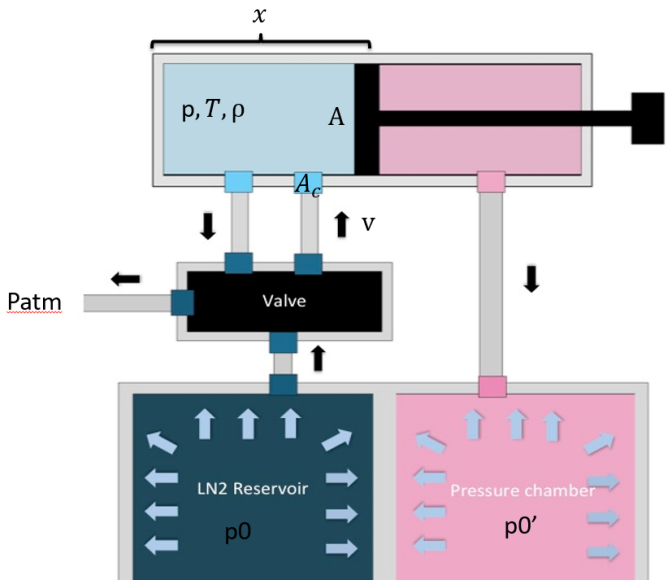

Figure 1 Liquid nitrogen powered pneumatic piston

The parameter we want to control is piston position x, and the control input is valve opening A_c (positive for inlet, negative for outlet), there are 4 intermediate parameters, p, T, ρ inside the chamber, and inlet/outlet velocity v. Our job is to relate x to A_c, thus we need four equations to solve intermediate parameters.

In order to come up with the equation, we list our assumptions here.

1. The flow is adiabatic, this means there is no heat transfer through the wall of chamber.
2. The flow is isentropic, this means there is not viscosity, no heat transfer, no shock wave along the flow. From this assumption, we can reach the conservation of enthalpy.

3. The flow is incompressible. Note here it doesn't mean the density is not changing. It only means the density of the flow 1, so the density inside the chamber is the same as it is in the reservoir. But since we are changing x (compressing the gas), the density will change over time.

First, let us take the control volume as the left chamber, and consider the first law of thermodynamics.

$$\frac{d}{dt}\int \rho\left(u+\frac{v^2}{2}+gz\right)dV+\oint \rho\left(u+\frac{v^2}{2}+gz\right)\underline{u}\cdot\underline{n}dS=\dot{Q}-\dot{W} \tag{1}$$

The first term on the left hand side signifies the change of internal energy inside the chamber. Let us ignore the gravity of gas, and assume that the gas is quiescent inside the chamber. Then the total energy of the gas is given by:

$$U=Mu=\rho VC_vT=C_vpV/R \tag{2}$$

where u is the specific internal energy (internal energy per unit mass). From thermodynamic properties we have:

$$u=C_vT \tag{3}$$

And the third equality is given by the ideal gas law inside the chamber

$$\mathrm{p}=\rho\mathrm{RT} \tag{4}$$

The second term is the inlet flow of energy, which can be written as,

$$\oint \rho\left(u+\frac{v^2}{2}+gz\right)\underline{u}\cdot\underline{n}dS=-\dot{m}\left(u+pv+\frac{v^2}{2}\right)=-\rho A_cv\left(u+pv+\frac{v^2}{2}\right) \tag{5}$$

where $\dot{\mathrm{m}}=\rho\mathrm{A_c v}$ is the inlet flow rate.

Due to the adiabatic assumption, we can assume $\dot{Q} = 0$. $\dot{W}$ is the work done by the system to the surroundings, which is piston work in our system. Now we have:

$$W = p\dot{V} \tag{6}$$

Let the pressure in the right chamber be p'. Then we have the equation of motion for piston:

$$(p - p')A = m\ddot{x} + b\dot{x} \tag{7}$$

Equation (7) gives the complete dynamics of our plant, which is necessary to design a proper controller.

Note that system is not only highly nonlinear, but also highly coupled, which means that it is extremely challenging to linearize the system, if at all possible. Also, the coupling may make the system to behave in an unpredictable way. Although equations (1) to (6) describe the thermodynamic phenomenon inside the vessel, due to the limitations in linearizing this system of equations, we picked a sample pressure for the controllers. Also, we try several different types of controllers, from standard PID to more complicated adaptive controller or fuzzy controller, to see how they work out.

Methods and Results

PID Control

All control design development is done in simulation using Simulink, Matlab. With the knowledge of pressure dynamics evaluated in the previous section, we can compute the force input to the actuator using the following equation (7), where m and b are mass and friction of the pneumatic piston, respectively.

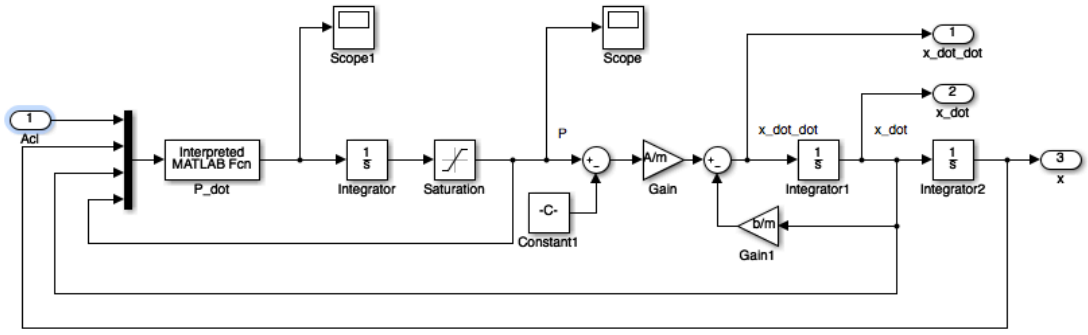

Figure 2 Plant set up

A standard PID controller was designed to test our plant (figure 4).

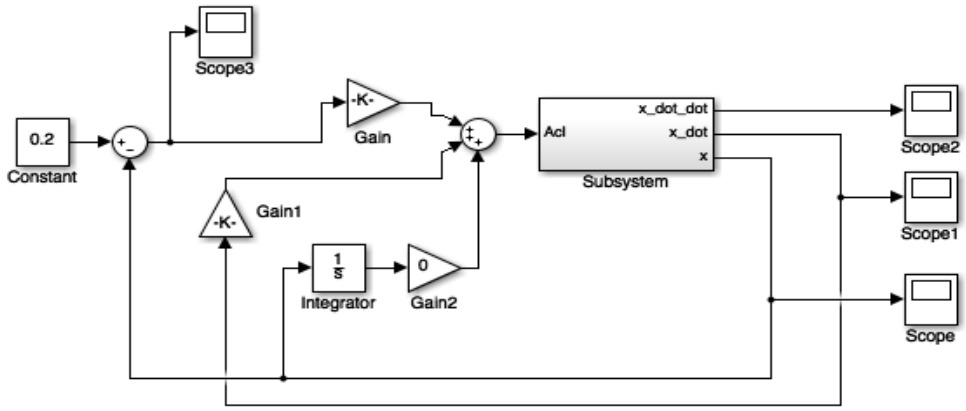

Figure 3 PID controller

We initially used 1 kg mass piston to run the controller and found out that the system would never be stabilized (figure 5, video ref. “small_mass.avi”). The response time of the plant is too fast even for the controller with gains as high as Kp = 10^6 and Kd =10^5 (Ki = 0 because the error build up would be too high).

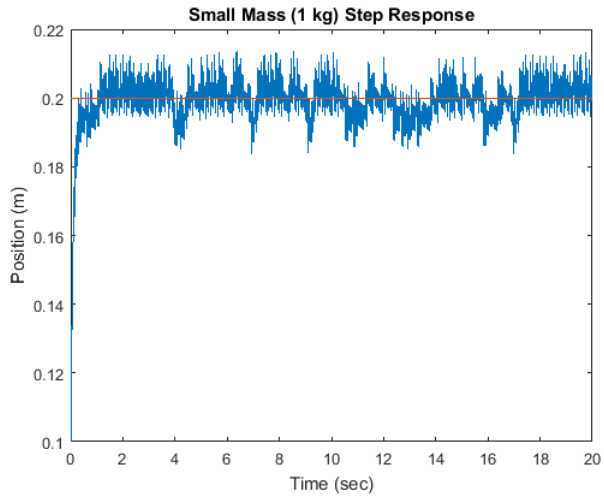

Figure 4 PD controller step response (m = 1 kg)

To slow down the time response of the plant, we decided to increase the mass of the piston, since the increased inertial force felt by the actuator allows the controller to have more effect on the system. With 200 kg mass piston, we could actually get a stable step response with reasonable values of gains (Kp = 2000 and Kd = 1000) (figure 6, video ref. “large_mass.avi”).

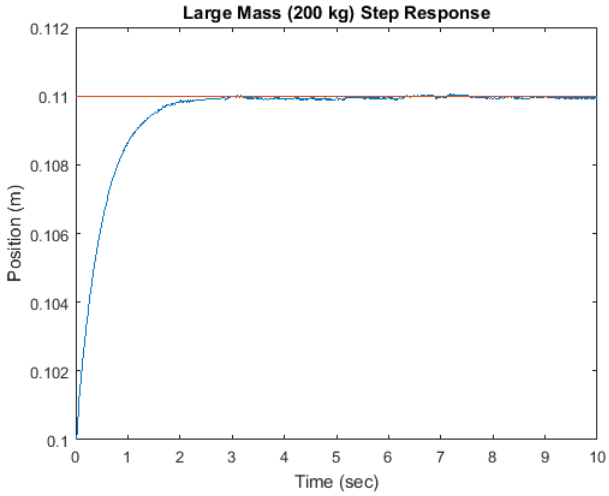

Figure 5 PD controller step response (m = 200 kg)

To test the controller robustness, we took a step back to our pressure dynamics derivation (p_dot), where we made a number of assumptions. One of the assumptions is that the reservoir pressure (p0) stays constant because we have an infinite amount of source. Such assumption can easily be disrupted in reality due to

gas leakage, delay in LN2 injection, and other non-ideal behaviors of the gas. We tested our controller for different reservoir pressures (figure 7).

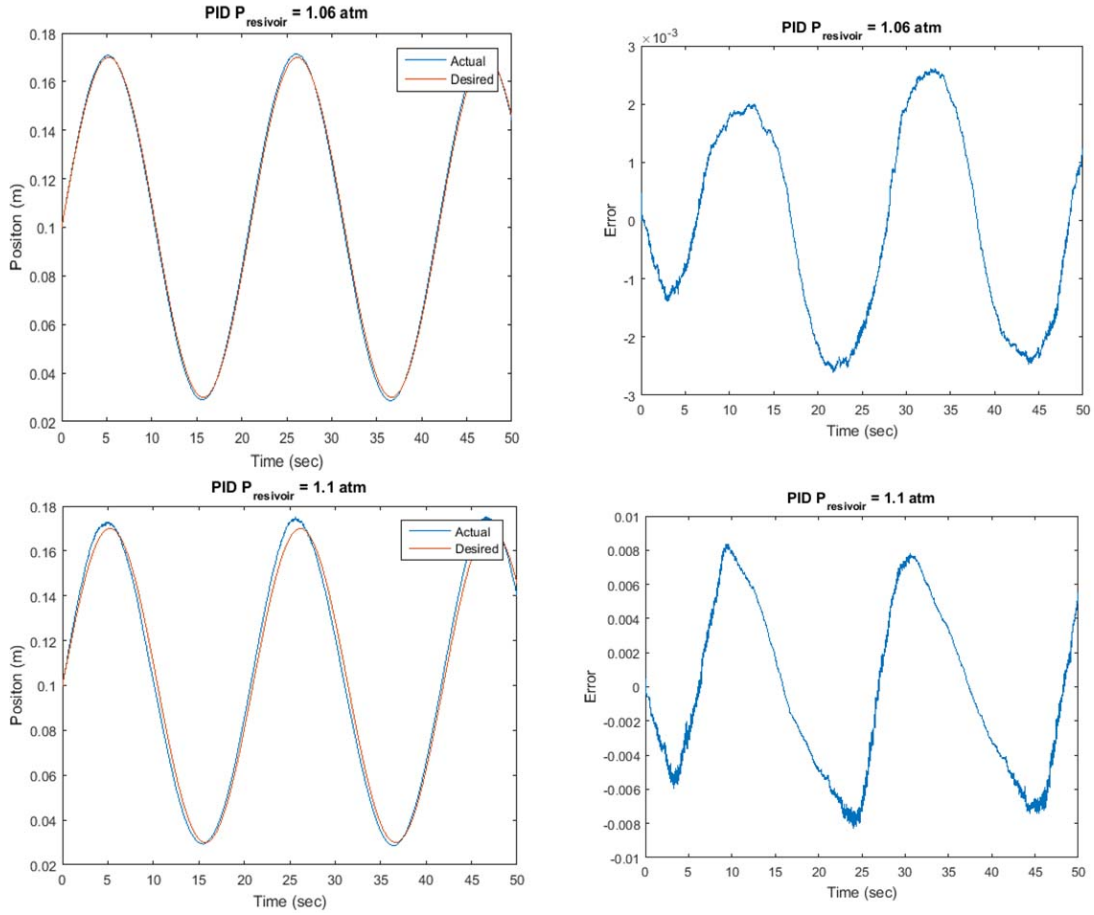

Figure 6 PID robustness testing. with different reservoir pressure (P0)- Position tracking with P0 = 1.06 atm (top left), position error with P0 = 1.06 atm (top right), position tracking with P0 = 1.1 atm (bottom left), and position error with P0 = 1.1 atm.

As shown above, the PID exhibited lower performance for reservoir with higher pressure. Gain tuning was necessary for better performance, which led us to believe that some kind of parameter adaptation strategy should be added our controller.

Adaptive Control

Adaptive control described by Craig in [1] is used to adjust the inverse dynamics of the controller to account for poorly estimated constants. In [1] Craig performed a simulation on a two-link manipulator. The idea behind his adaptive controller for the two-link manipulator is as follows. The equations of motion for a two-link manipulator can be written in the form

$$\tau = M(\theta)\ddot{\Theta} + Q(\Theta, \dot{\Theta}) \tag{8}$$

And the control law using inverse dynamics is

$$\tau = M(\theta)(\ddot{\Theta}_d + K_v\dot{E} + K_pE) + Q(\Theta, \dot{\Theta}) \tag{9}$$

Where

$$E = \theta_d - \theta$$

Equating (13) and (14) leads to

$$\ddot{E} + K_v\dot{E} + K_dE = 0 \tag{10}$$

Equation (15) shows that if we know our system perfectly then we can drive the error to zero and have perfect performance. However in the real world we do not know our system perfectly so our control law is actually

$$\tau = \widehat{M}(\theta)(\ddot{\Theta}_d + K_v\dot{E} + K_pE) + \hat{Q}(\Theta, \dot{\Theta}) \tag{11}$$

Where $\widehat{M}$ and $\hat{Q}$ represent the estimates of the system. Now using this new control law equating (13) and (16) leads to

$$\ddot{E} + K_v\dot{E} + K_dE = \widehat{M}^{-1}(\Theta)[\,\widetilde{M}(\theta)\ddot{\Theta} + \tilde{Q}(\Theta, \dot{\Theta})] \tag{12}$$

Where

$$\widetilde{M}(\theta) = M(\Theta) - \widehat{M}(\Theta) \;\; and \;\; \tilde{Q}(\theta) = Q(\Theta) - \hat{Q}(\Theta)$$

It is clear from (17) that we can no longer drive the error to zero. The adaptive controller presented by Craig is used to minimize the right hand side of equation (17). In his paper Craig proves that if the appropriate update function is used then it is guaranteed that the right hand side of equation (17) will be minimized. The update function that is proposed is in the form of

$$\dot{\hat{P}} = \Gamma W^T \widehat{M}^{-1} E_1 \tag{13}$$

Where P is a column vector of all constants that get updated, Γ is a square matrix of arbitrary gains, W includes all parameters that scale each constant as they show up in the equations of motion, and $E_1 = \dot{E} + \alpha E$. Where α is chosen so that the following transfer function is strictly positive real

$$\frac{s + \alpha_j}{s^2 + k_{vj}s + k_{pj}}$$

In order to understand adaptive control, Craig's two-link manipulator simulation was reproduced with the following method. Figure 8 and Figure 9 show the Simulink used to simulate the adaptive controller.

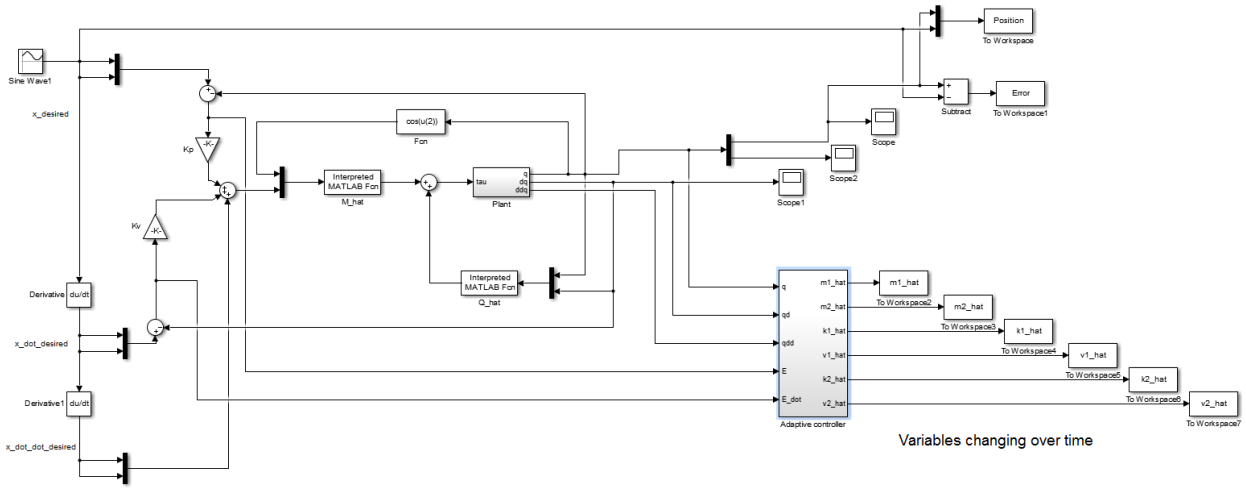

Figure 7 Adaptive control Simulink for a two link manipulator

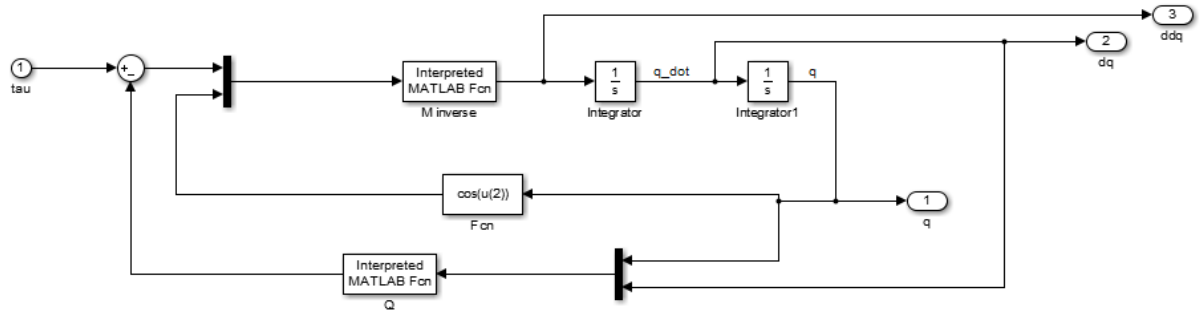

Figure 8 Plant Simulink model for adaptive controller

The actual constants used for this simulation were $m_1 = 4$, $m_1 = 4$, $m_2 = 4$, $l_1 = 1$, $l_2 = 1$, $v_1 = 6$, $v_2 = 4$, $k_1 = 10$, $k_2 = 10$, and $g = 9.81$. All equations of motion can be found in Craig [1] equation (41). The parameters that were used for the update function were as follows:

$$P^T = (m_1 \quad m_2 \quad k_1 \quad v_1 \quad k_2 \quad v_2)$$

$$\Gamma = \begin{bmatrix} 50 & 0 & 0 & 0 & 0 & 0 \\ 0 & 50 & 0 & 0 & 0 & 0 \\ 0 & 0 & 50 & 0 & 0 & 0 \\ 0 & 0 & 0 & 50 & 0 & 0 \\ 0 & 0 & 0 & 0 & 50 & 0 \\ 0 & 0 & 0 & 0 & 0 & 50 \end{bmatrix}$$

$$\alpha = 35$$

$$K_p = 1000$$

$$K_v = 100$$

The W matrix that was used was exactly the same as the W matrix found in Craig [1] equation (43). Using these constants and a sinusoidal position input produced the results shown in Figure 10 to Figure 12.

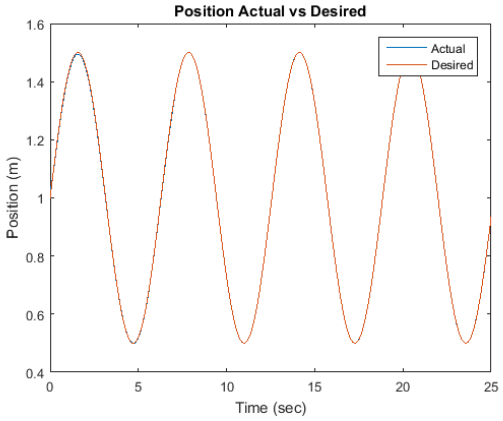

Figure 9 Positon input actual position, adaptive controller turned on at 7 seconds

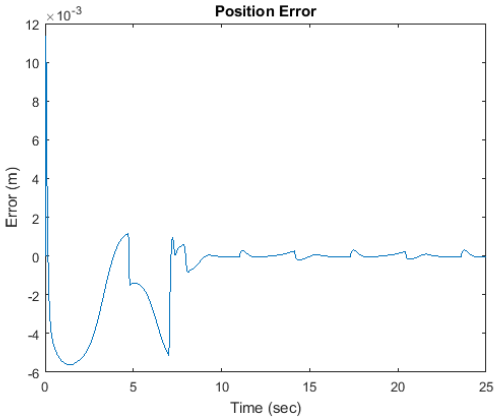

Figure 10 Position error, adaptive controller turned on at 7 seconds

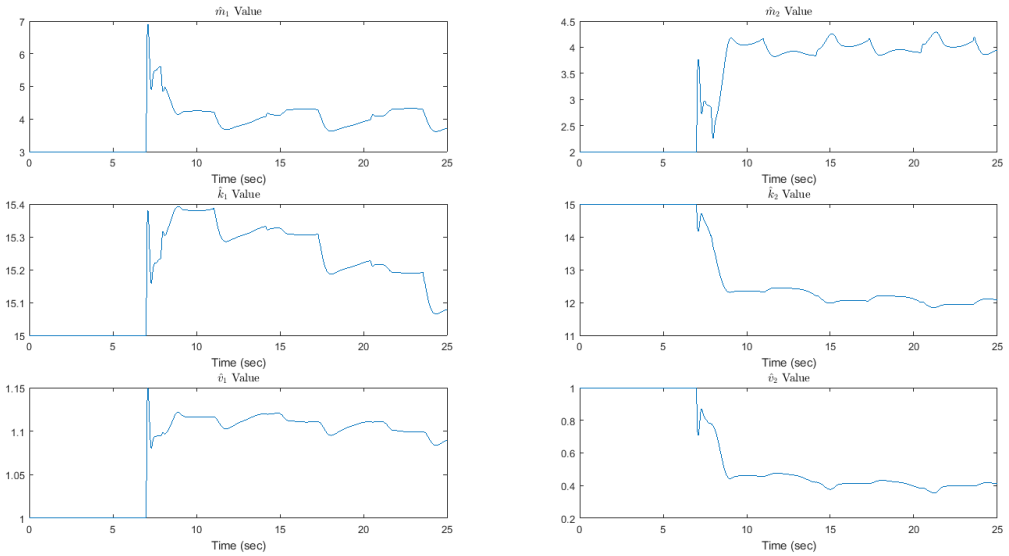

Figure 11 Update of estimates, adaptive controller turned on at 7 seconds

The adaptive controller is turned on 7 seconds and it is clear from Figure 11 that the error is minimized in a very short amount of time. What is more interesting is that the adaptive controller converges to steady state values for all of the constants but they are not what the real values are. Both the mass constants find the actual values but the spring and damping constants are not very close to the true values.
From these results we can conclude that we can successfully reproduce Craig's adaptive control method. Unfortunately after learning this technique we found that we are not able to implement this scheme on our plant. The reason for this is because we cannot separate our equations of motion into a nice for like equation Figure 13. Our control input is coupled to our plant dynamics making it impossible to isolate on one side of the equation, because of this we cannot use inverse dynamics. Therefore, we decided to use a fuzzy logic adaptive controller, which lends itself to our type of nonlinear plant.

Fuzzy Logic Adaptive Control

A fuzzy logic adaptive controller adjusts the PID gains rather than constants in the inverse dynamics. This type of controller lends itself to our nonlinear plant where it

is impossible to perform inverse dynamics. The control scheme used is described in [6] where an update function is used to update the proportional gain and the integral gain of the PID controller. The update function is as follows

$$\dot{K}_p = K_p + \vartheta e\mu \tag{14}$$

$$\dot{K}_i = K_i + \vartheta e\delta \tag{15}$$

Where ϑ is an arbitrary gain, e is the error, and μ and δ are values that are either 0 or 1. The values of μ and δ are decided using the following logic.

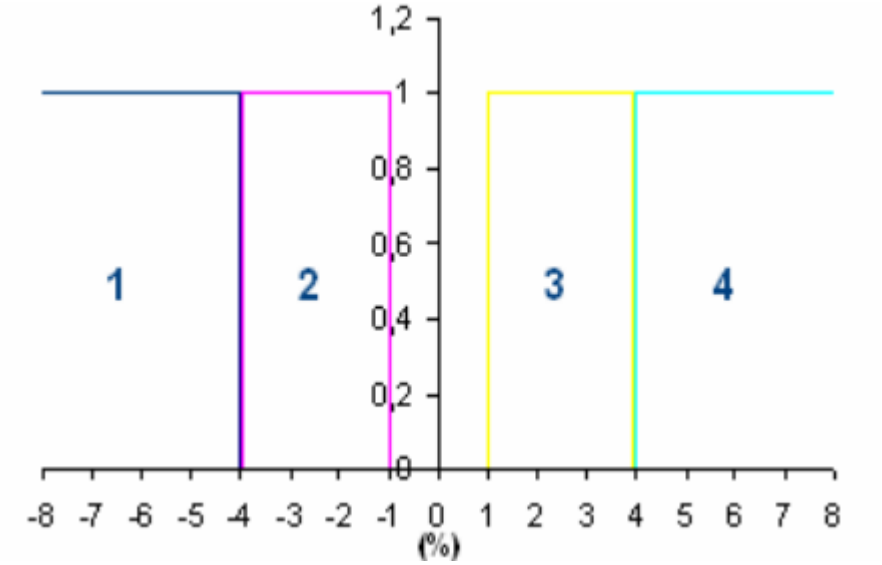

Figure 12 Fuzzy logic distribution and type of membership function

Figure 13 show that when the magnitude of the percent error is above 4% then $\mu = 1$ and $\delta = 0$ thus only the proportional gain will be adjusted. When the percent error is between 1%-4% then $\mu = 0$ and $\delta = 1$ thus only the integral gain will be adjusted, and finally when the percent error is less than 1% then both values are zero and no gains are adjusted. The intuition behind this control scheme is that if you have a large tracking error then you proportional gain needs to be increased to make the controller more aggressive. Once the tracking error is small enough adjusting the integral gain will get rid of any steady state error. We implemented a fuzzy logic controller using $\vartheta = 2000$ for the propotional update and $\vartheta = 100$ for the integral update. Figure 14 shows the Simulink used for the simulation.

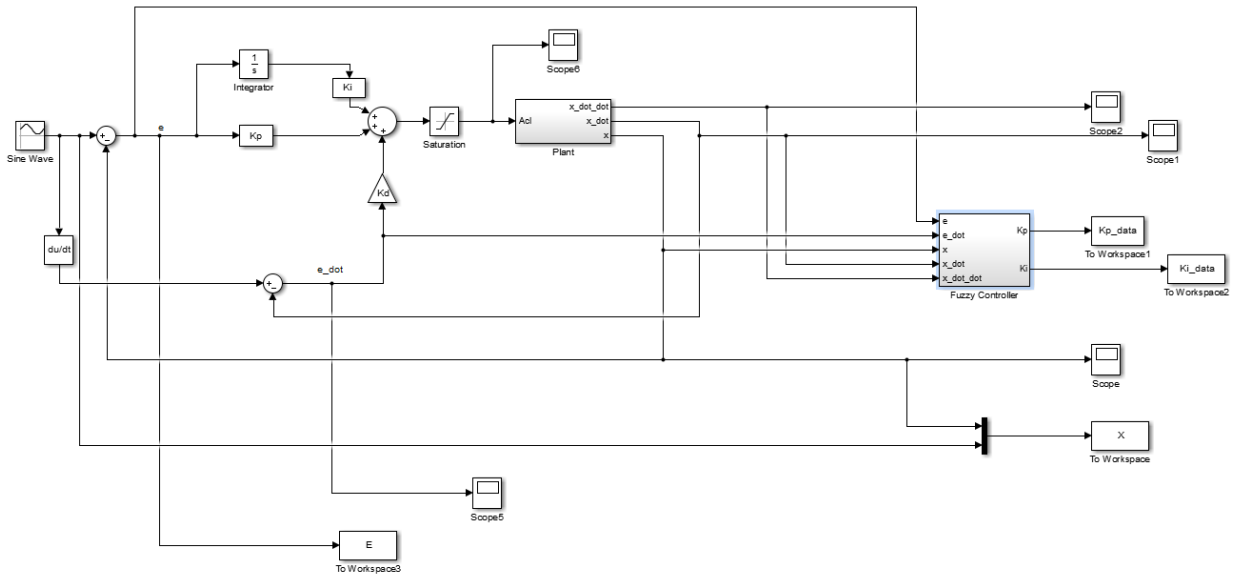

Figure 13 Simulink of system with fuzzy controller

Previously, we saw that the reservoir pressure would have a large effect on our system performance if the pressure of the reservoir were not a constant. We then applied the above fuzzy logic controller to try to counter act this problem. The results can be seen in Figure 15, please note that the fuzzy controller was turned on at 15 seconds (video ref. “fuzzyLogic.avi”).

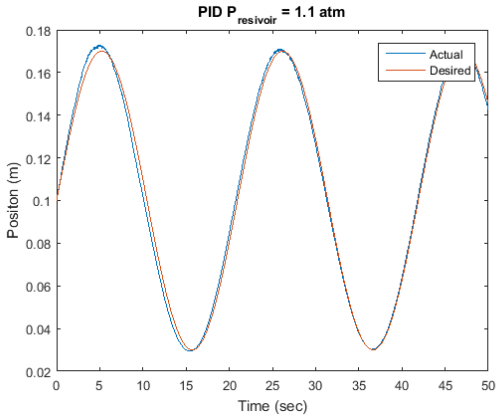

Figure 14 Position of piston, fuzzy controller turned on at 15 seconds

Pressure vessel experiment

Set-up

While the pneumatic piston design shown in figure 1 is used to confirm the validity of LN2 powered pneumatics system control problems, constructing exactly the same apparatus is both unrealistic and impractical. The infinite LN2 source assumption needs to be reconsidered. Also in real life, it is typically challenging to have an ideal valve that can handle a cryogen with a high pressure. As such, a simplified version of pressure vessel that can simultaneously function as a LN2 reservoir is newly designed and manufactured.

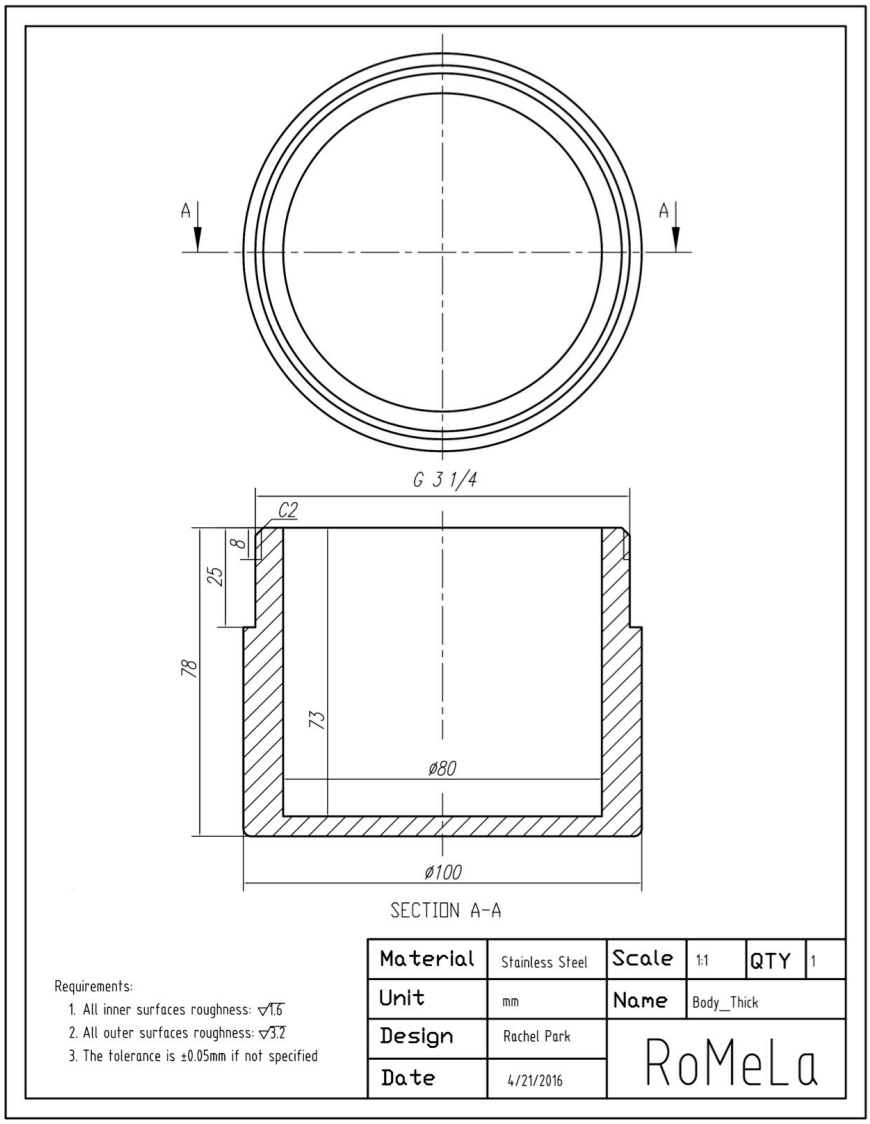

Figure 15 Pressure vessel body

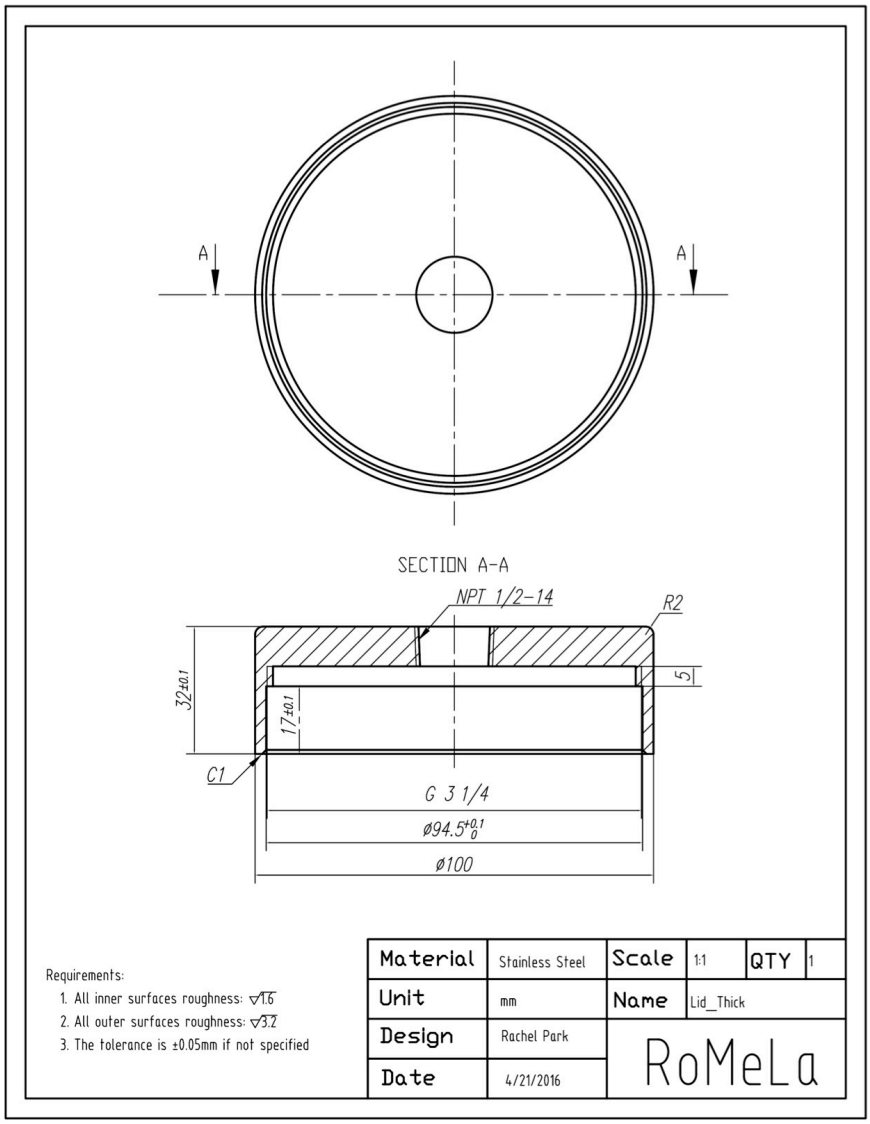

Figure 16 Pressure vessel lid

After some design iterations to make the vessel easy to implement in real life, we arrived at the design specified in in Figure 16 and 17. The outer diameter and the outer height are both 100 mm, with the lid closed. The vessel can withhold about 377mL of expanded gas nitrogen. The pullout strength of the lid threads is about 13455 N-m. The vessel is roughly 3 kg in mass and it is assumed to be able to handle a specific heat of 1472 J/K. With this design, we do not need the expensive cryogen-specific or the high-pressure-specific valves.

Procedure

1. Set up the customized pressure vessel with a generic pressure gauge and a control valve. Figure 18.
2. Prepare LN2 – from the LN2 reservoir, withdraw small amount (~200mL) to the transfer vessel using transfer hose. Figure 19.
3. Pour 30 mL to the Styrofoam cup
4. Place it inside of the pressure vessel
5. Close the lid and flip the vessel upside down
6. LN2 starts to evaporate immediately and rapidly as it touches the stainless steel wall of the vessel. Pressure builds up inside of the vessel. Figure 20.
7. At 0.5 atm gauge pressure, slowly release the valve and obtain pressure readings

Figure 17 LN2 experiment set up

Figure 18 LN2 withdrawal from the LN2 reservoir to the transfer vessel

Figure 19 Pressure reading after inserting 30 mL of LN2 and letting it completely evaporate inside of the vessel

Results

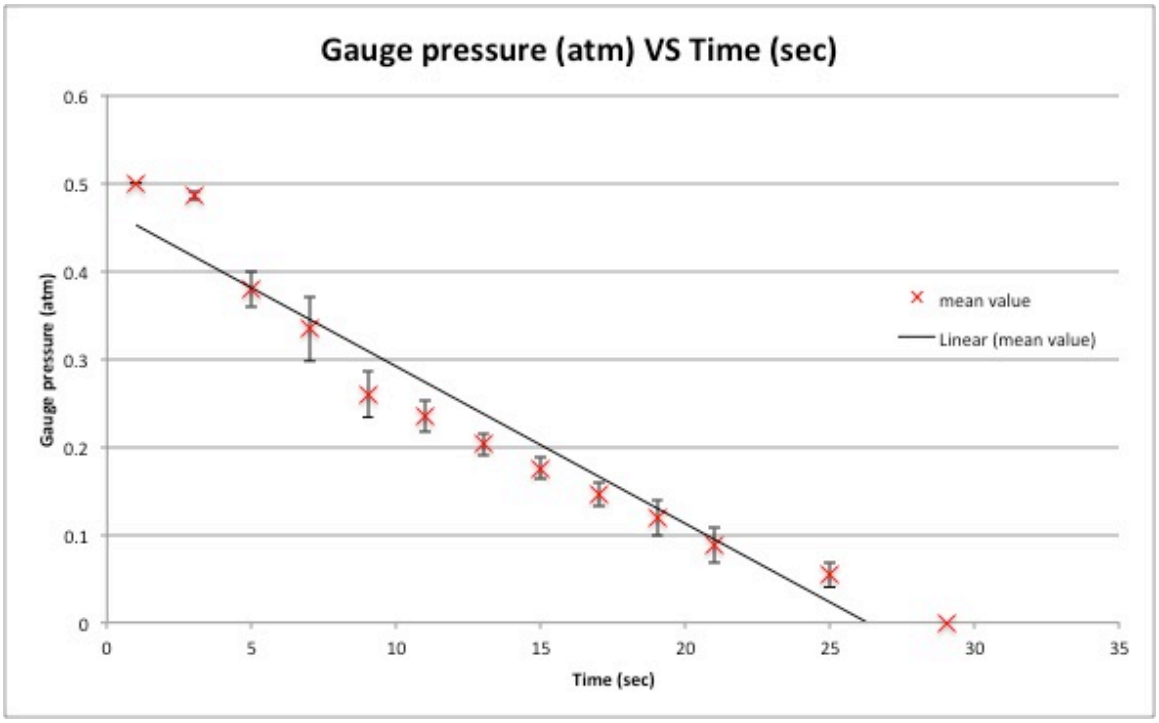

Figure 20 Pressure vessel gauge pressure vs. time

As shown in figure 21, the pressure vessel containing 30mL LN2 initially exerts 0.5 atm gauge pressure, which is exhausted in 30 sec exhibiting linear trend. Since 0.5 atm is equivalent of approximately 50 kN/m^2, we could confirm that this pressure vessel has a potential to supply enough power to a range of typical pneumatic muscle actuators for its operation for some limited amount of time. Some of its suitable applications include upper limb actuation systems for lightweight humanoid or exoskeleton robots.

Future works

For the simulation, our plant model is built upon a number of assumptions and ideal parameter selections. While most of them remain as reasonably viable choices, a couple of them appear to be less reliable than others. One of the more unreliable ones includes the incompressible gas assumption. We need to improve the plant model to take the compressibility of gas into account. In [7] suggests a method to construct a controller that incorporates gas compressibility by dividing the pressure dynamic into two conditions: the “choked” and the “under-choked”, for closed valve and open valve systems, respectively. We can also test different types of actuators besides piston, such as nozzles. We still believe that it’s better to utilize this power source as a “disposable” form than a “reusable” form, because compressing the exhausted nitrogen gas back to its liquid form is inefficient. Exploring other types of controllers, especially in nonlinear control regime, is also desirable. We can start expanding our control paradigm by introducing more control parameters, such as heat transfer inside of the vessel. As we obtained some pressure readings from the customized pressure vessel of our design, we can now construct a number of different types of pneumatic muscle actuators with step input pressure of about 0.5 atm.

Resources

Simulink, Matlab 2015a

Appendix

A. Notations

$p0$ – Pressure inside the reservoir

T_0 – Temperate inside the reservoir

h_0 – Specific enthalpy inside the reservoir

C_v – Specific heat at constant volume

C_p – Specific heat at constant pressure

R – Specific gas constant for nitrogen

ρ – Density of liquid nitrogen inside the left chamber

T – Temperate of liquid nitrogen inside the left chamber

p – Pressure of liquid nitrogen inside the left chamber

v – Inlet velocity of liquid nitrogen at the valve

u – Specific internal energy of liquid nitrogen inside the left chamber

M – Total mass of liquid nitrogen inside left chamber

U – Total internal energy of liquid nitrogen inside left chamber

V – Total volume of liquid nitrogen inside the left chamber

$\dot{Q}$ – Heat transfer into the liquid nitrogen inside left chamber

$\dot{W}$ – Work done be the liquid nitrogen inside left chamber on surroundings

A_c – Area of the inlet/outlet valve on left chamber

A – Area of the piston on both sides (assume identical)

x – Position of the piston

m – Mass of the load on piston

b – Friction coefficient of the piston

$p0'$ – Pressure inside the right chamber

p_{atm} – Atmosphere pressure

B. Heat transfer inside of the LN2 engine

Process of heat transfer accompanied by phase change is more complex than simple heat exchange between fluids since it concerns about not only thermodynamics, but also hydrodynamics. For our plant, we need to consider heat transfer during gas expansion followed by phase change of liquid nitrogen inside of the heat transfer vessel. The heat transfer coefficient of this process is not immediately known and can only be determined through experimentation. Fortunately, we are only interested in the range of plausible heat transfer coefficient values for the scope of this project. Using heat transfer coefficient of 1000 (red in the figure), for the dimension of vessel and amount of LN2 injection specified below, we confirmed that the temperature change inside of the vessel happens very quickly. As a result, we arrive to the conclusion that it is safe to assume that we have no time delay from this heat transfer process.

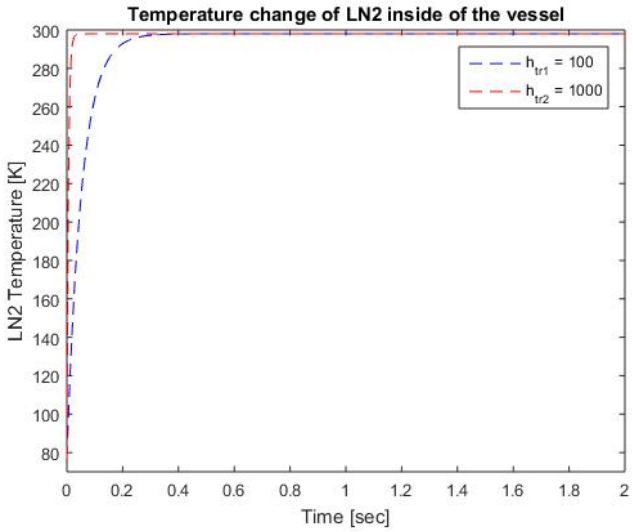

Figure 21 Temperature change of LN2 inside of the vessel

```
% Dimension of the heat transfer vessel
ro = 3.2; % [cm] outer radius
ho = 4; % [cm] outer height
ri = 3; % [cm] inner radius
hi = 3.5363; % [cm] inner height
c_steel = 460; % [J/kg-K;N-m/kg-K] Specific Heat Steel 430
```

```
% c_steel = 502; % [J/kg-K] Specific Heat Steel 304
c_n2 = 1.04e3; % [J/kg-K] Specific Heat Nitrogen
m_n2 = 3.228e-3; % [kg] mass of nitrogen
rho_steel = 7.8334e3; % [kg/m^3] density of steel
vol_steel = pi*((ro^2)*ho-(ri^2)*hi)*(10^-6); % [m^3] volume of the
steel vessel
m_steel = rho_steel*vol_steel; % [kg] mass of the steel vessel

% Heat Transfer
C_sys = (m_steel*c_steel+m_n2*c_n2); % combined mass specific heat
Temp_inf = 298; % [K] room temperature
h_tr = 1000; % [W/m^2-K;J/s-m^2-K] heat transfer coefficient
R_env = 1/(2*pi*ro*h_tr); % [m-K/W] environmental thermal resistivity
syms T(t)
DT = diff(T);
D2T = diff(T,2);
dsolve(diff(T) == (Temp_inf - T)/(R_env*C_sys),T(0) == 77)
t = linspace(0,5,1000);
T_f = zeros(1,length(t));
for i = 1:length(t)
    T_f2(i) = 298 - 221*exp(-(18014398509481984*t(i))/956429703554881);
% h_tf = 100
    T_f3(i) = 298 - 221*exp(-
(1152921504606846976*t(i))/6121150102751239); % h_tf = 1000
end
```

Bibliography

1. Craig, John J., Ping Hsu, and S. Shankar Sastry. ""Adaptive control of mechanical manipulators." ." *The International Journal of Robotics Research* 6, no. no. 2 (1987): 16-28.
2. Knowlen, Carl, A. T. Mattick, Adam P. Bruckner, and A. Hertzberg. ""High efficiency energy conversion systems for liquid nitrogen automobiles."." *SAE*, 1998: E6.
3. Li, Yongliang, Haisheng Chen, and Yulong Ding. ""Fundamentals and applications of cryogen as a thermal energy carrier: a critical assessment."." *International Journal of Thermal Sciences* 49, no. 6 (2010): 941-949.
4. Ordonez, C. A. ""Liquid nitrogen fueled, closed Brayton cycle cryogenic heat engine." ." *Energy Conversion and Management* 41, no. 4 (2000): 331-341.
5. Sharma, Atul, V. V. Tyagi, C. R. Chen, and D. Buddhi. ""Review on thermal energy storage with phase change materials and applications."." *Renewable and Sustainable energy reviews* 13, no. no. 2 (2009): 318-345.
6. Chaínho, João, et al. "A Simple PID Controller with Adaptive Parameter in a dsPIC; Case of Study." *Proceedings of the 9th Spanish-Portuguese Congress on Electrical Engineering*. 2005.
7. Kazerooni, H. "Pneumatic force control for robotic systems." *Mechatronics, 2004. ICM'04. Proceedings of the IEEE International Conference on*. IEEE, 2004.